Journal of Sedimentary Research

MICROBIAL BIOFACIES AND THE INFLUENCE OF METAZOANS IN HOLOCENE DEPOSITS OF THE LAGOA SALGADA, RIO DE JANEIRO STATE, BRAZIL

FRESIA RICARDI-BRANCO,[1] FLAVIA CALLEFO,[1] RAFAEL A. CATALDO,[1] NORA NOFFKE,[2] LUIZ CARLOS R. PESSENDA,[3] ALEXANDRE
C. VIDAL,[1] AND FABIO CARDINALE BRANCO[4]

[1]Department of Geology and Natural Resources, Geosciences Institute, P.O. Box 6152, Campinas University, UNICAMP, 13083-970, Campinas, SP, Brazil
[2]Department of Ocean, Earth and Atmospheric Sciences, Old Dominion University, Norfolk, Virginia 23529, U.S.A.
[3]Center for Nuclear Energy in Agriculture (CENA), Avenida Centenário 303, São Paulo University, 13416-000, Piracicaba, SP, Brazil
[4]Environmentality, Michigan, 177, 04566-000, São Paulo, SP, Brazil
e-mail: fresia@ige.unicamp.br

ABSTRACT: With the emergence of metazoans in the Neoproterozoic, microbialites have declined worldwide. Some hypotheses point to the direct activity of the metazoans, such as the predation of microorganisms that formed the microbial mats, as the reason for the decrease in the occurrence of microbialites since the beginning of Phanerozoic. However, this hypothesis is controversial due to the lack of direct evidence pointing to metazoan effects. Abundant subrecent microbialites and modern microbial mats occur in the Holocene lagoon Lagoa Salgada, Brazil, and its association with metazoans is remarkable. This contribution describes the various modern and fossil microbial biofacies and elucidates the paleoenvironmental evolution. It also investigates whether any interaction between the microbial communities and metazoans affected the morphology of the microbialites. Three biofacies were defined: (i) carbonate-cemented microbialites (CC), (ii) non-cemented planar microbial mats (NC-PM), and (iii) non-cemented cauliflower-shaped microbial mats (NC-CM). Biofacies (ii) and (iii) form biofilm catenae in the S and the SW margin of the lagoon, as a reflection of the current dynamics and relief of the lagoon. The microtextures of the biofacies are described in petrological thin sections analyses and X-ray microtomography. The mineralogy and elemental distribution were analyzed by SEM/EDS and μ-XRF. ^{14}C dating shows that the microbialites were established 2973–3383 cal. yr BP. During that time period the lagoon experienced a greater marine influence. Metazoans associated with microbialites and microbial mats include herbivorous, detritivorous, and opportunistic specimens. They occur filling voids and pores and also the fabrics of the microbialites and microbial mats. Although external factors such as the sedimentary evolution of the lagoon, the closure of the lagoon, its loss of connection with the sea, and the physicochemical changes during the whole process have caused prohibitive effects on the development of the microbialites, the metazoans appear to have a crucial effect on the framework of the bioconstructions, especially during the period with the greatest abundance of metazoans living in association with the microbial mats.

INTRODUCTION

According to Burne and Moore (1987), microbialites are organo-sedimentary deposits originated by trapping and binding detrital sediments by the action of a benthic microbial community. Microbialites occur in a wide range of environments, including open marine, freshwater, hypersaline, and even continental settings (Reid et al. 1995, 2003; Arp et al. 1999; Macintyre et al. 2000; Dupraz et al. 2004; Lopez-Garcia et al. 2005; Eckman et al. 2008; Gischler et al. 2011; Riding 2011; Hargrave et al. 2014). The environmental conditions for their formation usually include sufficient light to allow the photosynthesis and favorable temperature and water chemistry (availability of nutrients and ions necessary for the precipitation of calcium carbonate), conditions which allow the proliferation of the microorganisms, usually cyanobacteria (Pratt 1982).

Currently, there are many discussions about the influence of metazoans in the development of microbialites. After the explosion of multicellular diversity and the rise of Metazoa in the terminal Proterozoic, stromatolites

declined by predation and competition for space (Awramik 1971, 1991). The decline in abundance is attributed to grazing pressure and competition for space, among other effects such as physicochemical factors (Garrett 1970; Awramik 1971, 1982; Monty 1973, 1979; Riding 2006; Dupraz et al. 2009). However, there is no direct evidence for the hypothesis of influence by metazoans (Fedonkin 2003), which means a gap in understanding the effects of metazoan colonization on the microbial substrate.

Modern stromatolites are rare, and today they are more common in hypersaline settings (Riding 2011). In Brazil, they have been reported in hypersaline lagoons in Rio de Janeiro State, such as the Lagoa Vermelha (e.g., Vasconcelos et al. 2006; Spadofora et al. 2010; Delfino et al. 2012) and the Lagoa Salgada (Rodrigues et al. 1981; Srivastava 2002; Senra et al. 2006; Iespa et al. 2011; Silva e Silva et al. 2013; Birgel et al. 2015). In Lagoa Salgada, domal-shaped stromatolites (with thrombolitic mesostructure) and well-developed microbial mats are found forming various biofacies. In association with these biofacies numerous metazoans occur.

Its evolution is linked to a progressive loss of communication with the sea, with a regressive tendency that progressively altered the physical and chemical scenario during the development of microbialites (Martin et al. 1993; Coimbra et al. 2000; Dias and Kjerfve 2009; Birgel et al. 2015). Thus, the Lagoa Salgada offers a good opportunity to observe the effects of the paleoenvironmental evolution and the interaction with metazoans in the development of microbialites.

This study was carried out with the aims 1) to describe the biofacies of microbialites and microbial mats in the context of the evolution of the depositional setting in order to evaluate the effects of environment in its distribution, and 2) to evaluate any potential influence on development of microbialite and microbial mat by Metazoa.

STUDY AREA

Lagoa Salgada is located on the Cape of São Tome close to the town Campos in the northern part of Rio de Janeiro State (Fig. 1). It is part of the deltaic system of the Paraíba do Sul River (Srivastava 2002). The lagoon is approximately 7 km long and 1.5 km wide, with a maximum depth of 1–1.5 m at the time of the study. Srivastava (2002) and Silva e Silva et al. (2008) measured the average air temperature as between 28° and 31°C, and the average water temperature as about 27°C; they determined pH values of 8.2 to 9.7, electrical conductivity of 52.000 to 86.200 ms/cm, ranges of salinity of 4.2–6.4%, total CO_2 of 233.6 mg/l, and dissolved O_2 of 3.2 to 3.7 mg/l; the water composition includes 71.8 ppm calcium, 664 ppm magnesium, 8.846 ppm sodium, and 1.3 mg/l of silica in the form of quartz.

Quaternary Evolution

The evolution of the deltaic system of the Paraíba do Sul river was influenced by the presence of fan deposits coalescent from the Barreiras Formation, which were deposited at the end of the Pleistocene in semi-arid conditions and shallow water (Martin et al. 1993; Dias and Kjerfve 2009). These fans provided sediments for the subsequent formation of the delta plain. In the beginning of the Pleistocene, climate-related variations in sea level increased erosion of the continental deposits (Dias and Kierfve 2009). During the last glacial maximum (LGM), the regression of the coastline formed sandy terraces originated by the beach ridges. Before the end of glaciation, the rising sea inundated the coastal plains developed during the Pleistocene. As a consequence sandy barriers and four coastal lagoons formed which are known as the Mololô, Ostras, Flecha, and Lagoa Salgada (Martin et al. 1993). Some of them have been filled by eolian silt or they lost their connection with the ocean. The sandy barriers also modify the morphology of the nearby coast of the Cape of São Tomé. The Lagoa Salgada was formed 3,600 cal yr B.P., and the development of the microbialites seems to have started soon after its formation (Coimbra et al. 2000). This development may be related to a period of drier climate than today (Toledo et al. 2009).

METHODS

Mapping the Lagoa Salgada by Remote Sensing

The distribution pattern of microbialites and microbial mats in the Lagoa Salgada was mapped with QuickBird satellite images taken on March 26th, 2004 and on August 8th, 2009. Field visits were in October 2009, May

2010, September 2010, and October 2011. Fifty sampling sites were chosen (Fig. 1).

The distribution of the microbial communities in the Lagoa Salgada was mapped by orbital remote sensing. ERDAS Image® and ArcGIS® software were used to identify areas with a typical photosynthesis response in the lagoon and its neighborhood (Fig. 2E), including areas with angiosperms.

Initially, the linear contrast stretching was made to improve the details visualization of the surface, using panchromatic bands, which presents the best spatial resolution. The Normalized Division Vegetation Index (NDVI) was employed, using the equation $(NIR - R)/(NIR + R)$; where NIR is near-infrared and R is red. This procedure assisted in determining the distribution of microbial mats in the extensive, and partly inaccessible, area of the lagoon and allowed a more targeted, time-saving approach. Afterward, the false-color composite images were made, using NDVI images in the red channel, the red band of the electromagnetic spectrum in green channel, and the green band in blue channel, in order to generate the image in Figure 2E. All of the images were subjected to linear contrast stretching highlighting, so that the areas where photosynthesis was taking place were highlighted in red. Also, the information was verified in the field in order to assure mapping accuracy and to match the images generated by ArcGIS® with in-site field observations.

Sampling

Samples were collected only in the NE, SW, and S margins, because these sites were accessible. In total 24 samples of microbialites, four samples of microbial mats, as well as eight samples of sediment were collected. Live specimens of invertebrates were also collected, such as microgastropods *Heleobia australis* d'Orbigny 1835, and specimens of crustaceans, such as the Tanaidaeae and Amphipoda, as well as Ostracoda. The invertebrates were fixed in 70% ethanol. By light microscopy, we identified the species according to the specific morphological character-istics of their appendices, body shapes, jaws, etc. These specimens were found inhabiting the margins of the Lagoa Salgada in association with living microbial mats (e.g., Ostracoda, microgastropods, foraminifera, among others) or loosely distributed in voids and cavities of the microbialites (e.g., foraminifera, ostracods, microgastropods, and crusta-ceans). They were compared with the specimens found firmly cemented within the framework of the microbialites. All samples are stored in the Paleontological Archives of the Institute of Geosciences of the State University of Campinas (UNICAMP).

Sample Preparation

In order to study the background sediments surrounding the micro-bialites, three groups of samples were taken (see Table 1 in Supplemental Material): i) loose sedimentary particles found in voids and cavities of 20 microbialites (13 for the NE side and seven for the SW side, Fig.1) were removed from the microbialites by shaking each entire microbialite in an individual sampling bag; ii) eight samples of background sediments surrounding the microbialites and microbial mats were taken; 10 cm^3 of each sample was separated for analysis; iii) sedimentary particles firmly incorporated into the matrix of microbial mats (four samples) and frames of microbialites (six samples) were extracted. In order to extract intra-mat sedimentary particles, the microbial mats were first dried in a dry oven and the grains manually removed. The mineral particles of all three sample groups (i–iii) were sieved and separated into three grain-size fractions (> 1

→

FIG. 1.—Study Area. **A)** Location of Rio de Janeiro State in Brazil. **B)** Location of the Lagoa Salgada in Rio de Janeiro State. **C)** Overview of Lagoa Salgada (QuickBird satellite image of March 26, 2004) and locations of the sampling sites (The number showing collecting sites of microbialites, microbial mats, and background sediments, indicated in the table in the supplementary material.
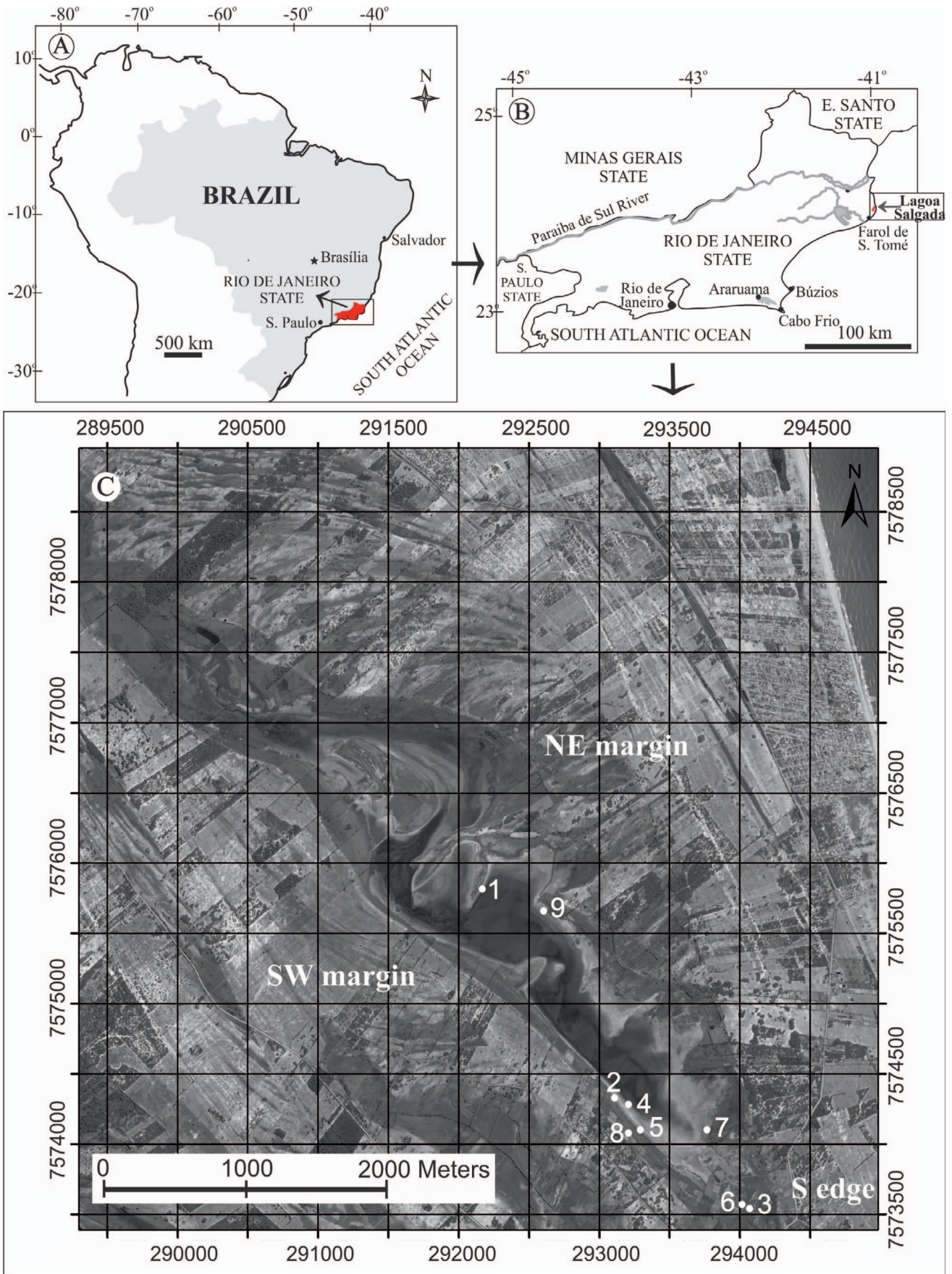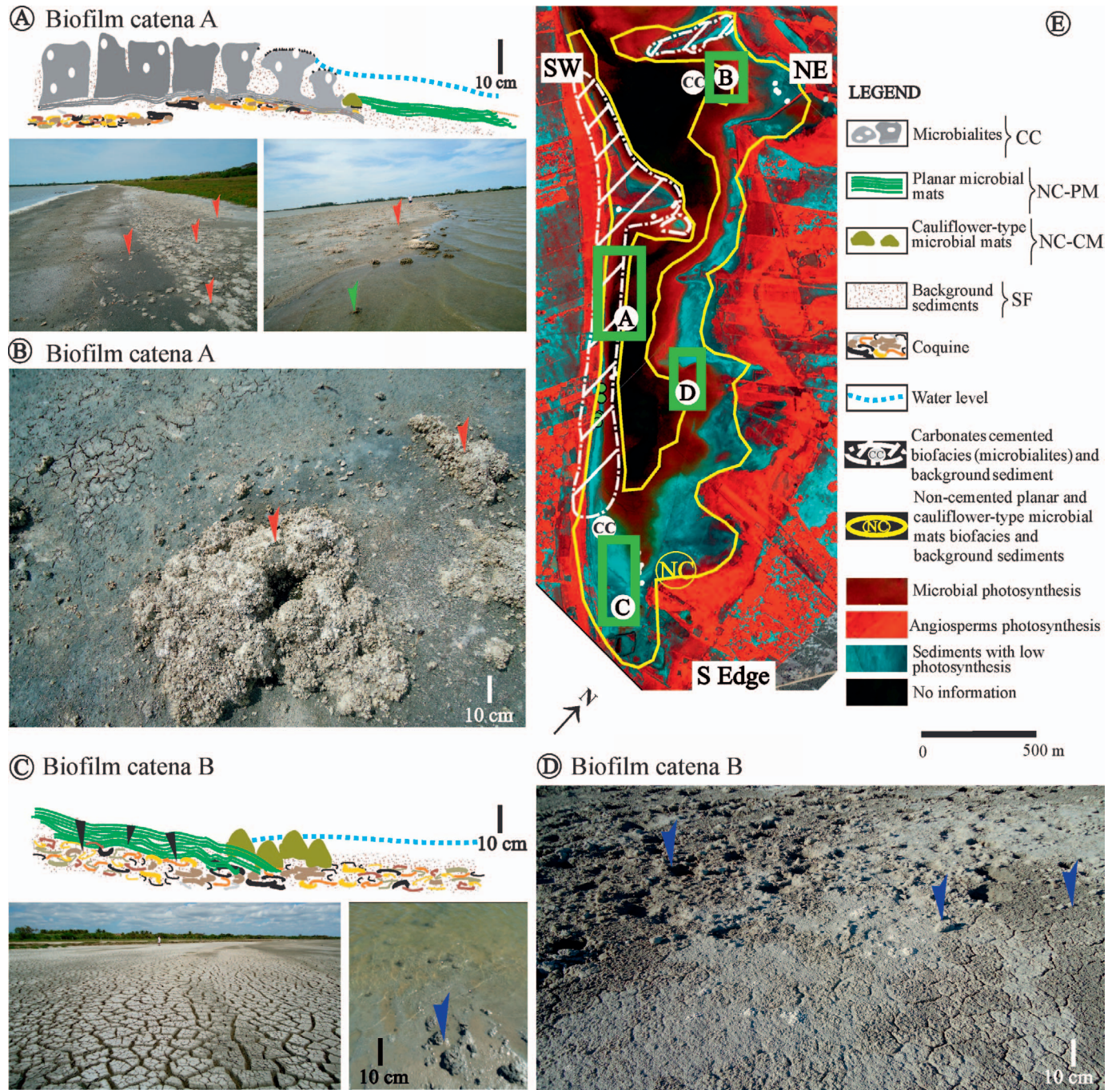
FIG. 2.—Distribution of the three biofacies proposed for the Lagoa Salgada. The green squares show the location of the transects detailed in Parts A, B, C, and D. **A)** Sketch of biofacies distribution in the SW-central area of the lagoon, corresponding to biofilm catena A: microbialites, cauliflower-type microbial mat, and planar microbial mat; the left photo below the sketch shows the carbonate-cemented biofacies (CC-microbialites, red arrows) embedded in the background sediments (SF); the right photo shows the non-cemented microbial mat biofacies (planar microbial mats, green arrow). **B)** Detail of the biofacies in the NE of the lagoon (CC, microbialites, red arrows). **C)** Sketch of biofacies distribution in the S edge of lagoon, corresponding to biofilm catena B; the left photo shows cracks in a non-cemented microbial mat (NC); the right photo shows cauliflower-type microbial mats (blue arrows). **D)** Detail of the biofacies in the NE of the lagoon (cauliflower-type microbial mats, blue arrows). **E)** Lagoa Salgada image in false color, using Normalized Division Vegetation Index (NDVI): areas of intense photosynthesis are shown in bright red. Locations of (CC) and (NC) are indicated as such.

mm, between 1 and 0.5 mm, and < 0.5 mm); the 105 fractions obtained were weighted.

Six microbialites were chosen for detailed investigation: three derived from the NE margin of the lagoon, and three from the SW margin (Fig. 1). In order to investigate their internal build-up, six microbialites (Fig. 1) were cut perpendicularly into two halves. Formerly trapped and bound

sedimentary grains were scraped out from selected internal laminae of each of the microbialites.

All of the samples were separated into 2 categories: skeletal grains (biogenic origin) and non-skeletal grains (inorganic minerals, formed by physical and/or chemical processes).

TABLE 1.—^{14}C dating and $\delta^{13}C$ of microbialites of the Lagoa Salgada.

Samples/Zone	Laboratory Identification	Age (years BP)	Age Calibration (yr 2σ)	$\delta^{13}C$ (‰)
CP6/10B, basal	CEN1189	2340 ± 80	2290–2548	0.47
CP6/22, upper	CEN1188	1990 ± 80	1771–2145	17.84
CP6/22, intermediate	CEN1186	2250 ± 80	2038–2370	12.96
CP6/22, basal	CEN1187	3020 ± 80	2973–3383	2.08
CP6/23, upper	CEN1185	2000 ± 80	1771–2151	13.41
CP6/24, upper	CEN1184	1970 ± 80	1726–2120	10.11

Microfacies Analysis

With a ZEISS stereoscopic microscope Stemi 2000-C, the skeletal grains were further separated into microgastropod shells (because these were extremely abundant), and other skeletal grains. Other metazoan organisms such as encrusters were studied in the field.

In order to study the microfacies, thin sections oriented perpendicular to the intra-microbialite laminae were made. The thin-section analysis was performed at IG-UNICAMP, at the Paleohydrology Laboratory, with a petrographic microscope Scope A1 ZE/SS (Carl Zeiss). The images were recorded with ZEISS AxioCam and treated at ZEISS's AxioVision® 4.8.2.0. (2006) software. They were analyzed using a petrographic light microscope. Also, SEM/EDS (energy dispersive spectroscopy) was employed for mineralogical composition analysis (Fig. 1). SEM/EDS analysis was performed at the Spectroscopy and Scanning Electron Microscopy Laboratory (MEV-IG-UNICAMP), using the SEM equipment LEO430i (LEO Electron Microscopy Ltd.) coupled to EDS equipment (Oxford Instruments), through the digital scan of the thin sections controlled by the software Labbok (Carl Zeiss). The analyses were performed by using the SEM equipment at room temperature, and the thin sections were covered with carbon coating. The semiquantitative analyses were made using the SEMQuant software (Link ISIS, Oxford Instruments, version 3.35) with ZAF corrections (Z-correction for atomic number, A-correction of X-ray absorption by the sample and F-correction of X-ray fluorescence production by X-ray generated by the sample). The ZAF correction was applied four times to generate the final result, which consists of the elementary percentages for each shot.

According to Birgel et al. (2015), the uppermost laminae of the microbialites record changes in the physicochemical conditions in the Lagoa Salgada. In order to study the distribution of the elemental concentration in the top of microbialites, elemental maps were made with μ-XRF analysis performed using the beamline in the Brazilian Synchrotron Light Radiation (LNLS). The samples were prepared by cutting a small block for performing elemental mapping. A microbialite sample was chosen that showed nice laminae in the top area (CP6/17, SW edge). The beamline was used in micro-beam mode with the KB focusing system to reach a beam size of approximately 12 × 25 mm, in air and at room temperature. The excitation was made in white-beam mode to ensure maximum flux. The data were treated and the semi-quantitative maps were performed using the PyMCA software (developed by European Synchrotron Radiation Facility-ESRF).

In order to describe microbial mats, a Skyscan 1272 X-ray micro-tomography analysis was performed in the Brazilian Nanotechnology National Laboratory (LNNano). For preparation, a 75 mm × 70 mm fraction of microbial mat was hardened in resin and cut to instrument fit. A nominal resolution of 350 nm was used, producing 2D and 3D images to show the internal microstructure of the microbial mats.

^{14}C Dating and $\delta^{13}C$

In order to obtain data regarding ^{14}C dating and $\delta^{13}C$ values, microbialites of both margins of the lagoon were analyzed (two samples in the NE (CP6/10a and CP6/10b) and three in the SW margin (CP6/22, 23, and 24). The sample CP6/22 was cut horizontally into three parts (basal, intermediate, and upper zone), in order to observe any change in results along the vertical extent of the microbialite. All samples were treated with 2% HCl to eliminate secondary carbonates, followed by washing with deionized water and drying in a dry oven (50°C). Organic remains were manually removed under the light microscope. Finally, the samples were milled, synthesized to benzene, and analyzed by liquid scintillation counting (Pessenda and Camargo 1991) at the ^{14}C Laboratory of the Centre for Nuclear Energy in Agriculture (CENA), University of São Paulo. Radiocarbon ages were normalized to a $\delta^{13}C$ value of –25‰ VPDB and reported as calibrated years (cal yr BP; 2σ) using the CALIB 6.0 and the SHCal13 curve.

The pre-treated samples were pulverized (50 mg) for analyzing $\delta^{13}C$ at the Chemistry Laboratory of ICP/MS of the Institute of Geosciences of USP in São Paulo, Brazil, using a continuous flow isotopic ratio mass spectrometer (CF-IRMS). ^{13}C results are given with respect to VPDB standard, using the conventional δ (‰) notation. Analytical precision is ± 0.2‰ (Saia et al 2008).

RESULTS

Biofacies Description

Three biofacies in the Lagoa Salgada are defined (Fig. 2E): the microbialites, which represent the carbonate-cemented biofacies (CC), the microbial mats, which represent the non-cemented planar microbial mats biofacies (NC-PM), and the non-cemented cauliflower-type microbial mats biofacies (NC-CM). Particles derived from the background sediments (SF) fill microbialite cavities or occur within the microbial mat fabrics.

Microbialites and microbial mats are widely distributed along the margin of the lagoon (Fig. 2A–D). They are responsible for the photosynthetic activity observed in the remote-sensing images (Fig. 2E). The remote-sensing images in Figure 2 show also the angiosperm vegetation that surrounds the lagoon.

Carbonate-Cemented Biofacies (CC), Macrofacies Analysis.—The 24 samples have a size range from 11 to 56 cm in length, and from 8 to 30 cm in width. The height varies from 14 to 16 cm. In vertical sections, the internal build-up of the microbialites is characterized by alternating dark and light laminae. The laminae are commonly convex upward with an occasional centimeters-wide wavy appearance (Fig. 3A, B).

On the NE margin of the lagoon, the microbialites generally developed on a firm ground formed by tubes of polychaetes (family Serpulidae); on the SW margin, the microbialites generally developed on firm ground composed of coquinas (Fig. 3E). In any case, the firm ground is considered here as part of the basal zone, because in some samples it is mixed with the firm ground. The vertical sections allow one to distinguish from base to top a threefold composition of the microbialites:

The basal zone (0.7 to 30 mm in thickness) consists of millimeter-scale, convex-upward laminae with intercalated small voids or pores varying from 0.5 mm to 0.5 cm, approximately, in size. Such a laminated pattern is typical for common stromatolites (Flügel 2004).

The intermediate zone (50 to 150 mm in thickness) overlies the basal zone, with an abrupt transition between them. In some samples, this zone is poorly preserved. The intermediate zone in well-preserved examples includes domes and/or branched structures (Fig. 3C, D), separated by broad voids partially or completely filled with quartz grains and bioclasts, including skeletal grains. It is possible to observe bioerosion marks in this zone. Voids ranging from 0.5 cm to 1.5 cm between the branches of
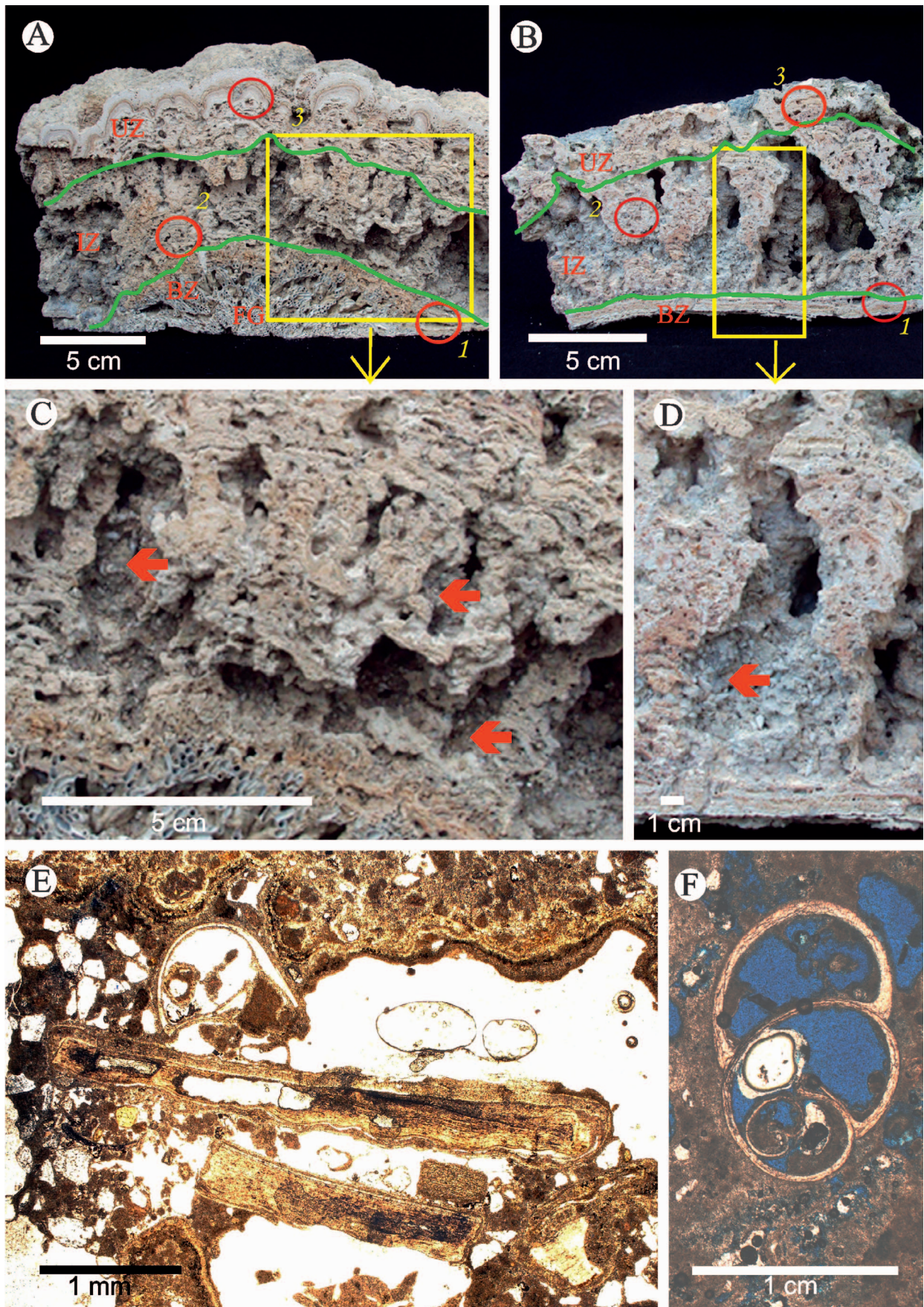
microbialites can also be observed (Fig. 3A–D). Therefore, this zone has a predominantly thrombolitic framework (macroscopically clotted fabric, Awramik 1982). This is in contrast to the basal zone, where stromatolite-like, convex-upward laminae are typical. Also, greater amounts of bioclasts among the grains retained in the matrix can be observed (Fig. 3F).

The upper zone is 20 to 30 mm thick. At the top of the intermediate layers, the microbialites expand and grow thicker. Also, their internal build-up changes from the clotted thrombolitic fabrics back towards the layered stromatolitic fabrics. Finally, at the very top, many microbialites join to form a plateau composed of laterally continuous planar to domal laminae with few voids. In comparison to the stromatolitic basal zone, the stromatolitic upper zone includes more branches and their structures are dominantly domal. Bioerosion is present, but less common than in the intermediate zone. A high density of encrusters (barnacles and bryozoans) generally conceals the pustular morphology of the top of the microbialite.

Carbonate Cemented Biofacies (CC), Petrographic Analyses.—The basal zone includes heterogeneous fenestral fabric, autochthonous micrite, microspar, and peloids. Isopachous rim needle cement of calcite occurs around cavities, quartz grains, and peloids. Most skeletal grains are fragmented only to a low degree; they are composed of foraminifera tests and mollusk and ostracod shells, commonly wrapped within a micrite envelope. The micritic coats are in turn fringed by isopachous calcite cements. The presence of fossil bivalves with both shell halves intact and closed indicates a low hydrodynamic level and little post-mortem transport. The skeletal grains sometimes have biocorrosion marks possibly caused by boring cyanobacteria. The dark-colored micritized peloids are rounded, ovoid or elongated, and present long-axis lengths from 31 to 600 μm. There are abundant circular cavities caused by bioerosion by activity of polychaetes, unfilled or partially filled by micrite.

The layers in the intermediate zone are more heterogeneous, but they contain many irregular cavities with sizes ranging from 0.5 mm to 0.5 cm, approximately; often they are partially filled by quartz grains, cemented by microspar (calcite and dolomite). Some skeletal grains and laminae are dominantly whole and show biocorrosion as a result of cyanobacterial and invertebrate activity (Fig. 4A). Peloids and isopachous rim cement layers occur around these cavities (Fig. 4B). Skeletal grains such as micro-gastropod shells (Fig. 4C), tests of foraminifera (Table 2), and ostracod shells, as well as encrusters such as bryozoans are visible. Since layering was incipient, skeletal grains, peloids, and minerals encased in micrite and microspar calcite cements were found. Quartz grains are corroded by cyanobacteria or micritized. Peloids are extremely abundant, usually dark brown with dimensions from 31 to 600 μm; sometimes they are amalgamated.

The upper zone is less friable than the basal and intermediate zones. The laminae are wavy, forming a fenestral fabric and laterally continuous (Fig. 4D, E). The skeletal grains, inorganic grains, and peloids have either a micrite envelope or isopachous rims; some examples, however, have both. The isopachous rim cement layers are also found around the cavities in the matrix. The skeletal grains, such as ostracod shells, are well preserved and were easily identified. Some microbialites have fenestrate fabric filled by peloids and quartz grains. In this upper zone of the microbialites, abundant bioerosion was observed: circular drillings of serpulids commonly filled by peloids and biocorrosion as a result of boring cyanobacteria (Fig. 4F).

Carbonate Cemented Biofacies (CC), Microfacies Analysis (SEM/ EDS and μ-XRF).—In the basal zone the SEM/EDS showed that the matrix is basically composed of low-magnesium calcite (point 1-LMC, Fig. 5A) and the firm ground below contains fossil tubes formed by polychaetes composed of calcite (point 2, Fig. 5A).

The SEM/EDS analysis indicates that the intermediate zone is strongly cemented by micrite LMC, but HMC and dolomite are present in lower percentages (Fig. 5B). The presence of some Mg clay, such as palygorskite, cannot be discarded. Magnesium ranges from none to 17%, mostly subordinate to calcium, however, it exceeds the calcium in some layers.

In the upper zone the μ-XRF maps for sample CP6 /17 from the SW edge (Fig. 5C), showed individual elemental distribution (Ca, Mn, and S) and spatial combination of the selected elements. The manganese occurs in the same area as calcium; the sulfur is distributed evenly in some laminae.

Non-Cemented Microbial Mat Biofacies (NC): Planar (NC-PM) and Cauliflower-Shaped Microbial Mat (NC-CM)

The two biofacies of microbial mats make up the non-cemented microbial mats biofacies (NC). Two types of microbial mat morphology were observed: 1) non-cemented planar microbial mats (NC-PM), which are microbial mats with horizontal to slightly wavy layers 0.5 to 10 cm in thickness and 2) non-cemented cauliflower-type microbial mats (NC-CM), which are cauliflower-shaped microbial mats that include, in vertical section, spheroidal-shaped "lenses" (instead of laterally continuous laminae) up to 10 cm in diameter.

Macroscopically, the NC biofacies are composed of a dark organic matter produced by the microorganisms and sediments. The EPS (extracellular polymeric substance) traps and binds inorganic sediments (non-skeletal grains) composed of quartz, clay, mica (mainly biotite), and calcite, and also a wide variety of bioclasts (skeletal grains, see Table 2). Both skeletal and non-skeletal grains are distributed within the organic matter and fill pores and voids in the two types of NC biofacies.

The NVDI images (Fig. 2E) showed areas around the lagoon with intense photosynthetic activity. The areas shown in different shades of red indicate photosynthesis by microbial mats and angiosperms (areas of plantations and natural vegetation outside of the lagoon). The microbial mats area (brownish red) reflects less photosynthetic activity than the angiosperm area due to the water, which absorbs part of the near-infrared radiation utilized in the NVDI calculation. The obtained NVDI images show that the non-cemented microbial mats are located around the entire lagoon, comprising all the margins, unlike the microbialites. Also, it is evident that the greatest extent of the microbial mats are on the S margin,

---

←

Fɪɢ. 3.—Framework of microbialites from the Lagoa Salgada seen in vertical sections. **A**, **B)** Microbialites along the NE and SW margin, showing basal level supported by serpulide communities (UZ, Upper zone; IZ, Intermediate zone; BZ, Basal zone; FG, firm ground; the numbers show where the sediments were taken from the matrix for analysis). **C)** Detail of the microbialite in Part A showing voids filled with sediments (red arrows). **D)** Detail of the microbialite in Part B showing voids filled with sediments (red arrows). E, F) Carbonate-cemented biofacies (CC): microfacies of basal zone of microbialite. **E)** Firmground composed of coquinas, microbialites of SW margin (CP6/ 25). **F)** *H. australis* shell partially corroded presenting intraparticle porosity surrounded by micrite (CP6/21).

→

Fɪɢ. 4.—Carbonate-cemented biofacies (CC). A, B, C) Microfacies of intermediate zone of microbialite. **A)** Bioerosion (red arrows) caused by invertebrates, partially filled with calcite (CP6/6A). **B)** Columns with thin layers with microspar, peloidal carbonate cements (red arrow), and isopachous rim cement (blue arrow) layers (CP6/6A). **C)** *H. australis* (blue arrows) shells in cavity, cross section (CP6/21). D, E, F) Carbonate-cemented biofacies (CC): microfacies of upper zone of microbialite. **D**, **E)** Columns cemented by micrite, wavy laminae, with a fenestral fabric and intact shells of ostracods (red arrow) in cavity (CP6/21 and CP6/6A). **F)** Peloids (red arrow) and biocorrosion (green arrow) (CP6 / 17B).
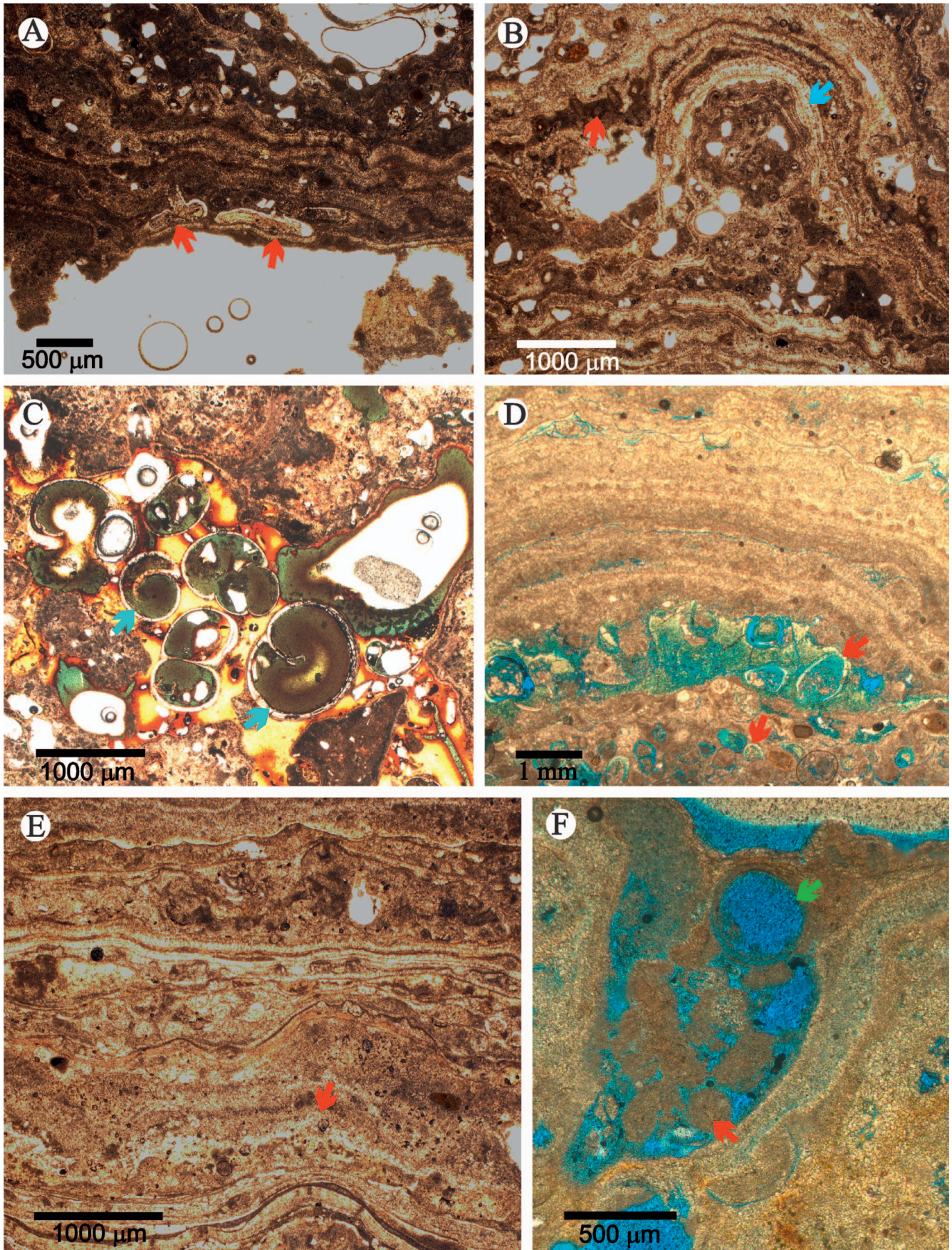
TABLE 2.—*Animals and plants distributed in microbialites, microbial mats, and sediments, Lagoa Salgada.*

	Biogenic Elements	Microbialite Voids		Microbialites Laminations		Microbial Mats		Background Sediments	
		(CC)	%	(CC)	%	(NC)	%	(SF)	%
FORAMS	*Quinqueloculina* sp.	X	2	X	5	X	6	X	11
	Ammonia sp.	X	0.1	X	0.8	X	0.6	X	2
	Elphidium sp.	X	0.04			X	0.35		
	Rosalina sp.	X	0.02						
	Triloculina sp.	X	0.02	X	0.2				
	Bolivina sp.	X	0.01			X	0.01		
	Miolliolinella sp.	X	0.1						
	Rotallina sp.	X	0.05						
	Textularia sp.	X	0.09						
	Cibicides sp.	X	0.01						
	Pseudonimion sp.					X	0.04		
ANELLIDA	Serpulids tubes	X	3	X	25				
MOLLUSCA	*Anomalocardia brasiliana* Gmelin, 1791	X	7	X	5	X	6		
	Helobia australis d'Orbigny, 1835	X	54	X	45	X	28	X	58
ARTROPODA	Ostracods	X	8	X	12	X	40	X	18
	Gammaridae carapaces	X	2						
	Tanaidaceae carapaces	X	5						
	Tanaidaceae tubular secretions	X	15						
	Carapaces of crustaceans	X	1			X	12	X	8
	Barnacles	X	2	X	5				
BRYOZOA	Bryozoan	X	0.36	X	2				
ECHINODERMATA	Spines of sea urchins							X	2
OSTEICHTHYES	Fish scales of *Tilapia* sp.							X	1
PLANTS	Carophytes (gyrogonites and twigs)	X	0.2			X	2		
	Talinum sp. (seeds)					X	5		

where there is the greatest exposure of wet sediment (but is not permanently flooded).

The X-ray microtomography analysis shows the 2D and 3D microstructure of the microbial mats (Fig. 6A). The distribution of bioclasts within the microbial mat layers can be observed, showing that several complete shells are distributed in specific layers of the mats—not randomly like other inorganic sediments. SEM/EDS analyses (Fig. 6A–I) show that the layered and spheroidal microbial mat layers include quartz grains and biotite and muscovite flakes, all contained in a fine matrix composed of dolomite, gypsum (Fig. 6C, D), HMC (Fig. 6F), halite (Fig. 6E, F), framboidal pyrite, and apatite (Fig. 6G, I). Both types of microbial mats include a fenestral texture and bioclasts (Table 2) such as foraminifera tests, microgastropod shells, ostracod shells, gyrogonites, charophyte stems, and seeds of *Talinum* sp. (Family Portulacaceae).

^{14}C Dating and $\delta^{13}C$ Analysis

The samples for $\delta^{13}C$ analysis and ^{14}C dating were collected from the SW and NE margin. As shown in Table 1, the oldest age was recorded in the basal zone of the CP6/22 microbialite (SW margin): 2973–3383 cal. yr BP ($\sim$ 3178 cal. yr BP). The other microbialites continued to develop for at least 1200 years (1726–2120 cal. yr. BP). The $\delta^{13}C$ values show variation in the development of the microbialites, with values beginning from 2.08‰ in the basal zone, and increasing to 12.96‰ in the intermediate zone until reaching 17.84‰ in the upper zone.

Background Sediments (SF)

In all samples of cemented biofacies (microbialite-CC) and microbial mat biofacies (NC), unconsolidated mineral and skeletal grains are concentrated in pores and voids. The sediments derive from the depositional background of the microbialites and microbial mats.

Detrital Mineral Grains.—Based on petrographic and EDS analysis, minerals composing the sediments are quartz, clay, mica (mainly biotite), and calcite. The quartz grains, sometimes with inclusions, varied from subrounded to subangular.

Skeletal Grains.—The sediments also include a significant amount of fragmented and complete shells and tests. Most abundant are foraminifera tests (Fig. 7A, B), bivalve shells (*Anomalocardia brasiliana* Gmelin 1791, Verenidae (Fig. 7C)), shells of microgastropods (e.g., *Heleobia australis* d'Orbigny 1835, Fig. 7D), carapaces of several crustaceans, such as of the order Tanaidaceae (Fig. 7E) and their semicircular tubular secretions (Fig. 7F), examples of the order Amphipoda (suborder Gammaridae, genus *Orchestia* (Fig. 7G), as well as of the class Ostracoda (?*Cipreides*, Fig. 7I), gyrogonites (Fig. 7H), and stems of carophyte *Talinun* sp. and seeds, appendices of other arthropods, bryozoan fragments, sea urchins spines, fish scales of *Tilapia* sp., and fragments of undetermined animal origin.

Table 2 shows the distribution and estimated percentage of each kind of bioclast in the three biofacies, including those found inside the matrix of microbialites and those found in voids and cavities. The data show that the

→

FIG. 5.—Carbonate-cemented biofacies (CC) analyzed in μ-XRF and SEM/EDS highlighting the selected elements and their distribution. **A)** Basal zone, eminence to the chemical composition of the matrix (red 1) consisting of LMC and Polychaeta tube (red 2) of calcite (LMC) composition; blue arrows showing quartz grains and yellow arrows rounded peloids (CP6/5 NE edge). **B)** Intermediate zone, green arrows showing *H. australis* and ostracod shells; blue arrow showing a quartz grain. Highlighting the chemical composition of the layers (red 1) and (red 2), with a layer of calcite (LMC) and (red 2) may consist of dolomite (CP6/SW edge 17). **C)** SEM image of upper zone, showing the area with μ-XRF maps with individual elemental distribution (Ca, Mn, S), and spatial combination of the selected elements (CP6/17 SW edge).
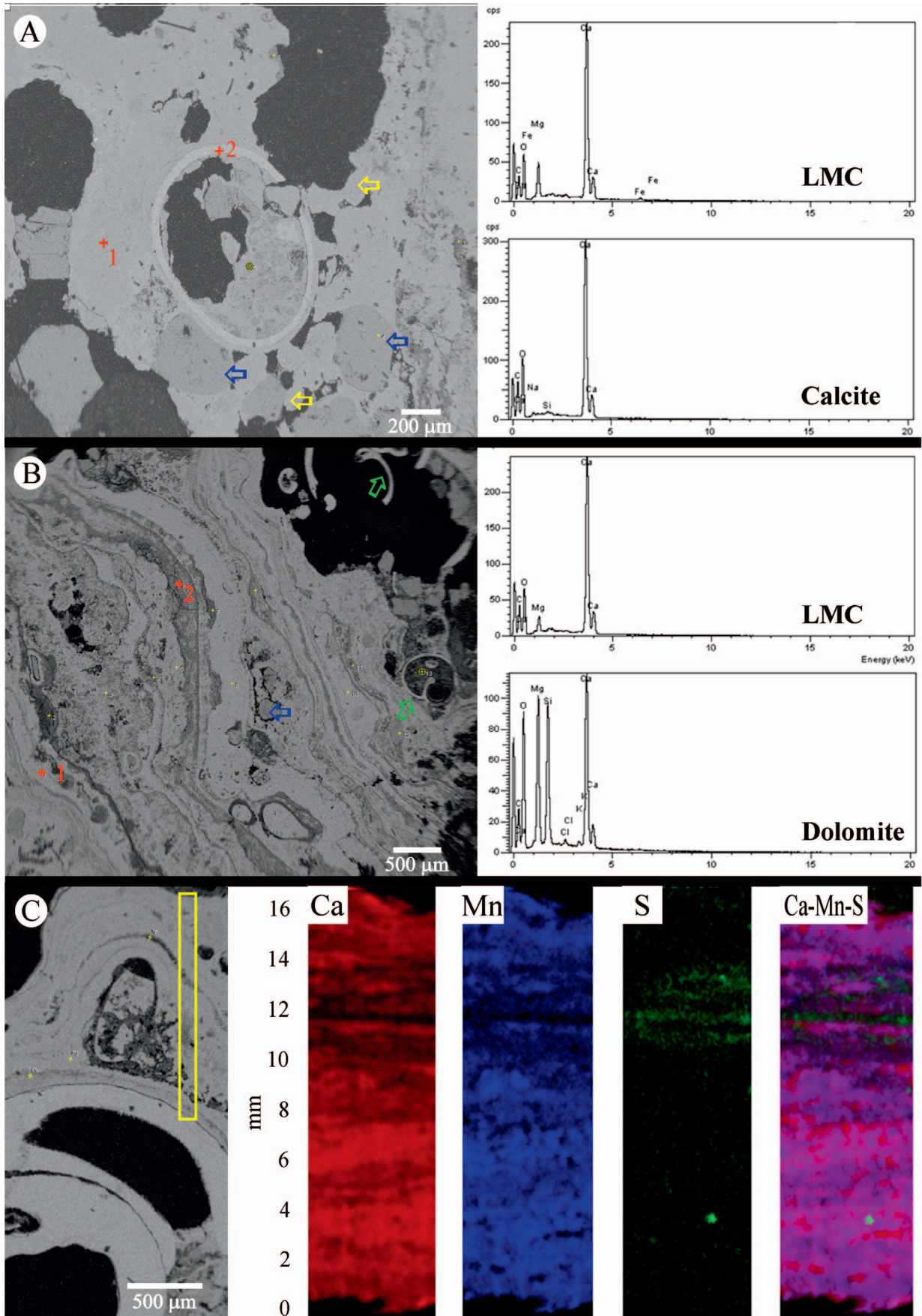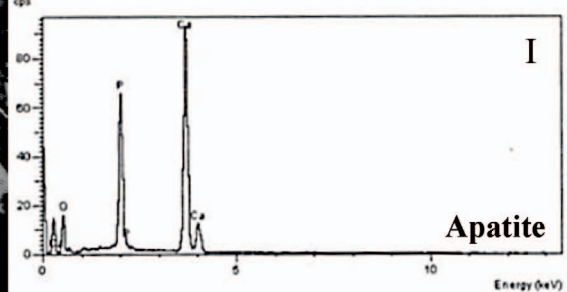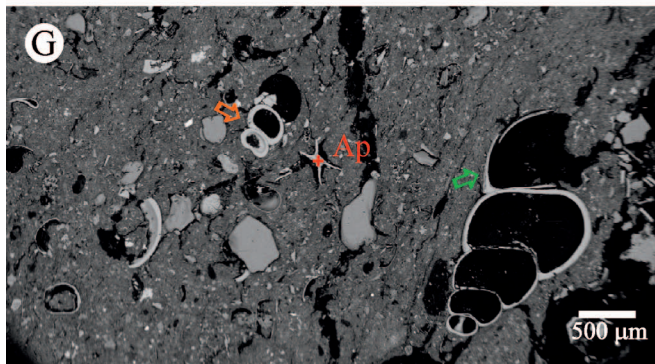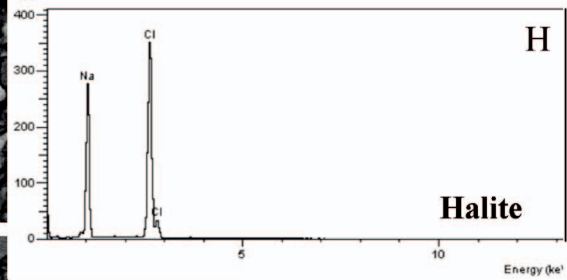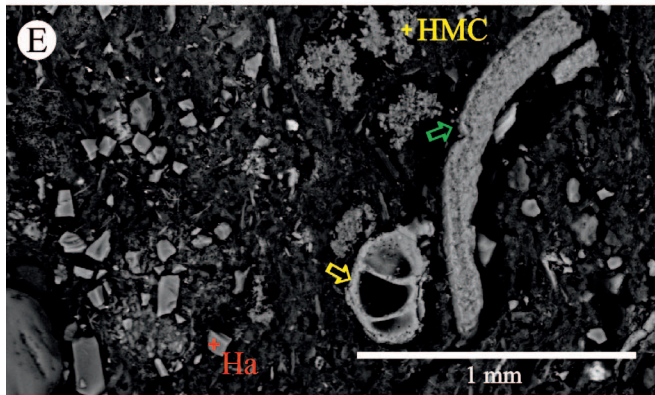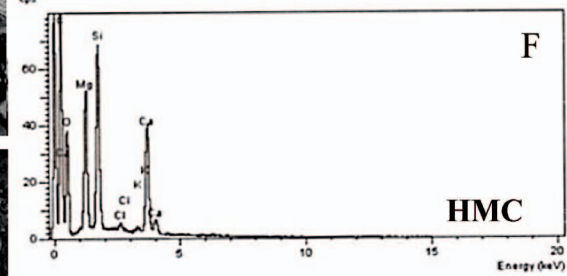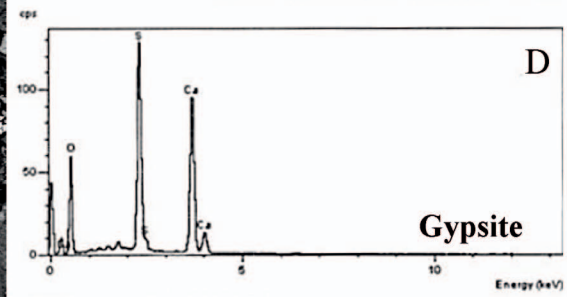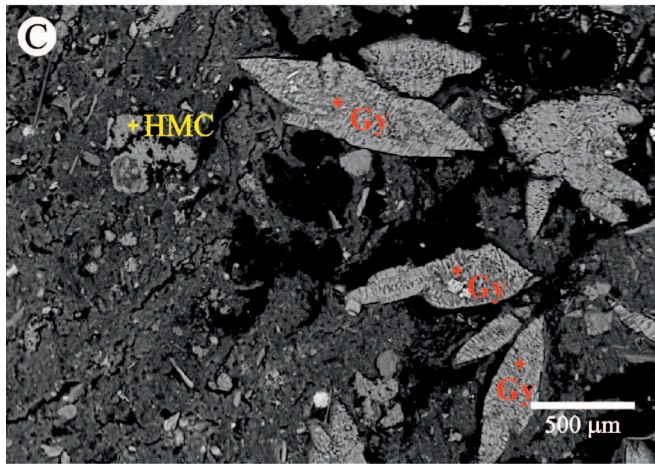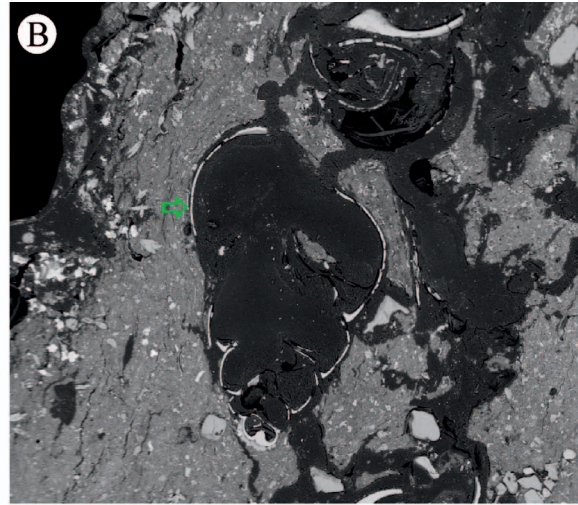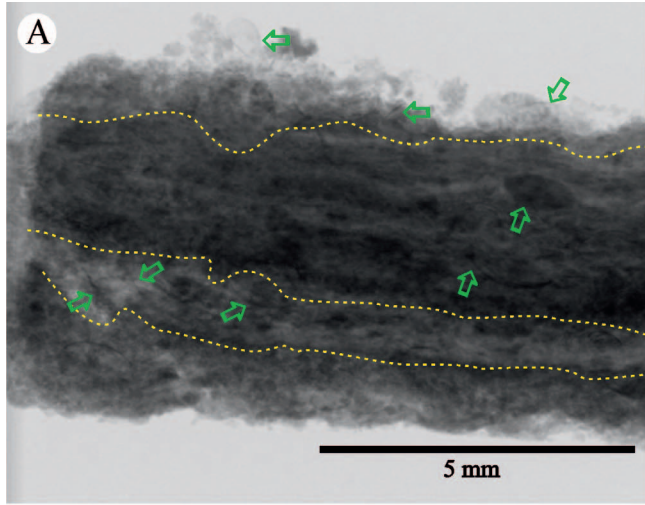
TABLE 3.—*Evolution of paleoenvironmental parameters of Lagoa Salgada during the development of basal, intermediate, and upper zones of microbialites.*

Zone	δ^{13}C (‰)	δ^{18}O (Birgel et al. 2015)	Framework of Stromatolites	Paleoenvironmental Configuration	Microbial Activity Predominance	Metazoan Abundance (*)
Upper	17.84		stromatolitic	closed lagoon with freshwater influence	methanogenesis	moderate
Intermediate	12.96	increase ↑	thrombolithic	transition to lagoon system	photosynthesis	high
Basal	2.08		stromatolitic	open marine	photosynthesis	low

(*) based on the proportion of bioclasts in relation of inorganic sediments, estimated by counting bioclasts and inorganic elements described in Methods section.

greatest diversity of bioclasts is filling the microbialites voids, especially foraminifera and some species of crustaceans (Gammaridae and Tanaidaceae). The most abundant (in percentage) elements in the microbialite voids are the Tanaidaceae tubes and the mollusk *Heleobia australis* d'Orbigny 1835, while in the microbialite laminae (inside the matrix), the most abundant element is the Serpulids tubes, the mollusk *Helobia australis* d'Orbigny, 1835 and ostracods, and less abundance of foraminifera in comparison with the voids and cavities. The microbial mats have more ostracods (more than microbialites) and also a high percentage of mollusks *Helobia australis* d'Orbigny, 1835 and carapaces of crustaceans. The background sediment is rich in *Helobia australis* d'Orbigny, 1835, ostracods, and the foraminifera *Quinqueloculina* sp. The composition of bioclasts is the same for both types of microbial mat (NC-PM and NC-CM).

Inorganic sediments are predominant in both margins, but the participation of microgastropods is also high. Figure 8 shows the abundance of bioclasts in the matrix of stromatolites on the SW and NE edges, both with the greater percentage in the intermediate zone of the microbialites.

DISCUSSION
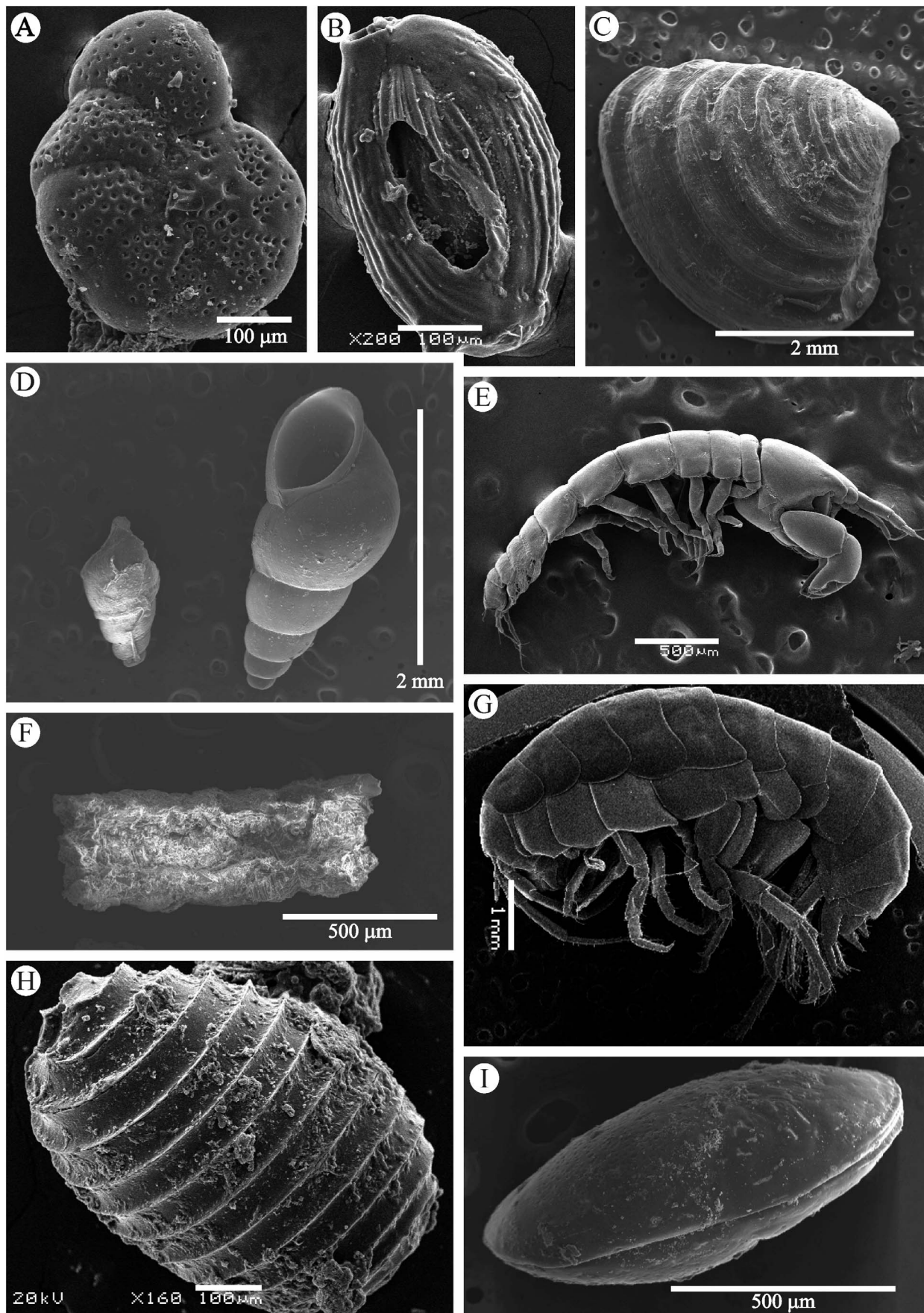
Paleoenvironmental Evolution

The development of the Lagoa Salgada is related to the evolution of the Paraíba do Sul River during the Holocene, and the sea-level variations during the past 7000 years BP (Martin et al. 1993; Dias and Kjerfve 2009). The Lagoa Salgada was formed 3600 yr BP (Coimbra et al. 2000) as result of deposition of submarine sand barriers. Several changes in physicochemical conditions and water level related to the regressive processes and progressive closure of the lagoon are reflected in the distribution of facies and framework of stromatolites. For the microbialites of the carbonate-cemented facies (CC, whose record begins at ~ 3178 cal. yr BP), three zones in their vertical development were distinguished (basal, intermediate, and upper zones) in this study. The paleoenvironmental changes and the consequences for the stromatolites are discussed below.

Basal Zone.—Based on ^{14}C data, the development of the microbialites (basal zone) began around 2973–3383 cal. yr BP (Table 1) in the SW margin, once forming an intertidal zone (Dias and Kjerfve 2009; Toledo et al. 2009). Based on δ^{13}C values from this study (2.08‰), and as suggested by Coimbra et al. (2000) and Birgel et al. (2015) with δ^{18}O data, the microbialites began to grow in conditions of an open marine environment (Tables 1, 3). The low value of δ^{13}C (2.08‰) of the basal zone is consistent with an open marine environment without microbial influence, which would increase the enrichment of ^{13}C of the stromatolite carbonate matrix. This occurs in the next two zones, in which an increase in δ^{18}O (Birgel et al. 2015) and δ^{13}C values can be observed. An earlier intertidal, marine influence is also suggested by the firmground (*sensu* Moore 2001) of tubiculous polychaetes (Serpulides) and bivalves (Verenidae). These

←

FIG. 6.—Non-cemented biofacies (NC-PM and NC-CM). **A)** NC-PM X-ray microtomography of longitudinal view of layered microbial mat including laminae of skeletal grains (highlighted in yellow). **B)** *H. australis* (green arrow) in microbial mat, shell filled by carbonate cement (calcite). **C)** Gypsite crystals (Gy in red) and high magnesium calcite (HMC in yellow) in microbial mats. **D)** Gypsite EDS spectra. **E)** Foraminifera tests (yellow arrow) and mollusk shells (green arrow); high-Mg calcite (HMC in yellow) in microbial mat, EDS spectra; halite crystal (Ha in red). **F)** High-Mg calcite EDS spectra. **G)** *H. australis* (green arrows) and apatite fish bones (Ap in red). **H)** Halite EDS spectra. **I)** Apatite EDS spectra relative to fish bones, shown in Part G.

→

FIG. 7.—Background sediments (SF): biota in microbialites from the Lagoa Salgada, SEM photography. **A)** *Quinqueloculina* sp. **B)** *Elphidium* sp. **C)** Shell of Verenidae. **D)** Shell of *H. australis*. **E)** Tanaidaceae. **F)** Tubes secreted by Tanaidaceae. **G)** Gammaridae. **H)** Charophyte gyrogonites. **I)** Ostracod carapace.

NE Edge

CP6/ 5

CP6/ 6

CP6/ 14

Upper Zone

13% / 87% 16% / 84% 18% / 82%

Intemediate Zone

33% / 67% 23% / 77% 35% / 65%

Basal Zone

5% / 95% 12% / 88% 6% / 94%

SW Edge

CP6/ 17

CP6/ 21

CP6/ 25

Upper Zone

13% / 87% 18% / 82% 15% / 85%

Intemediate Zone

32% / 68% 28% / 72% 43% / 57%

Basal Zone

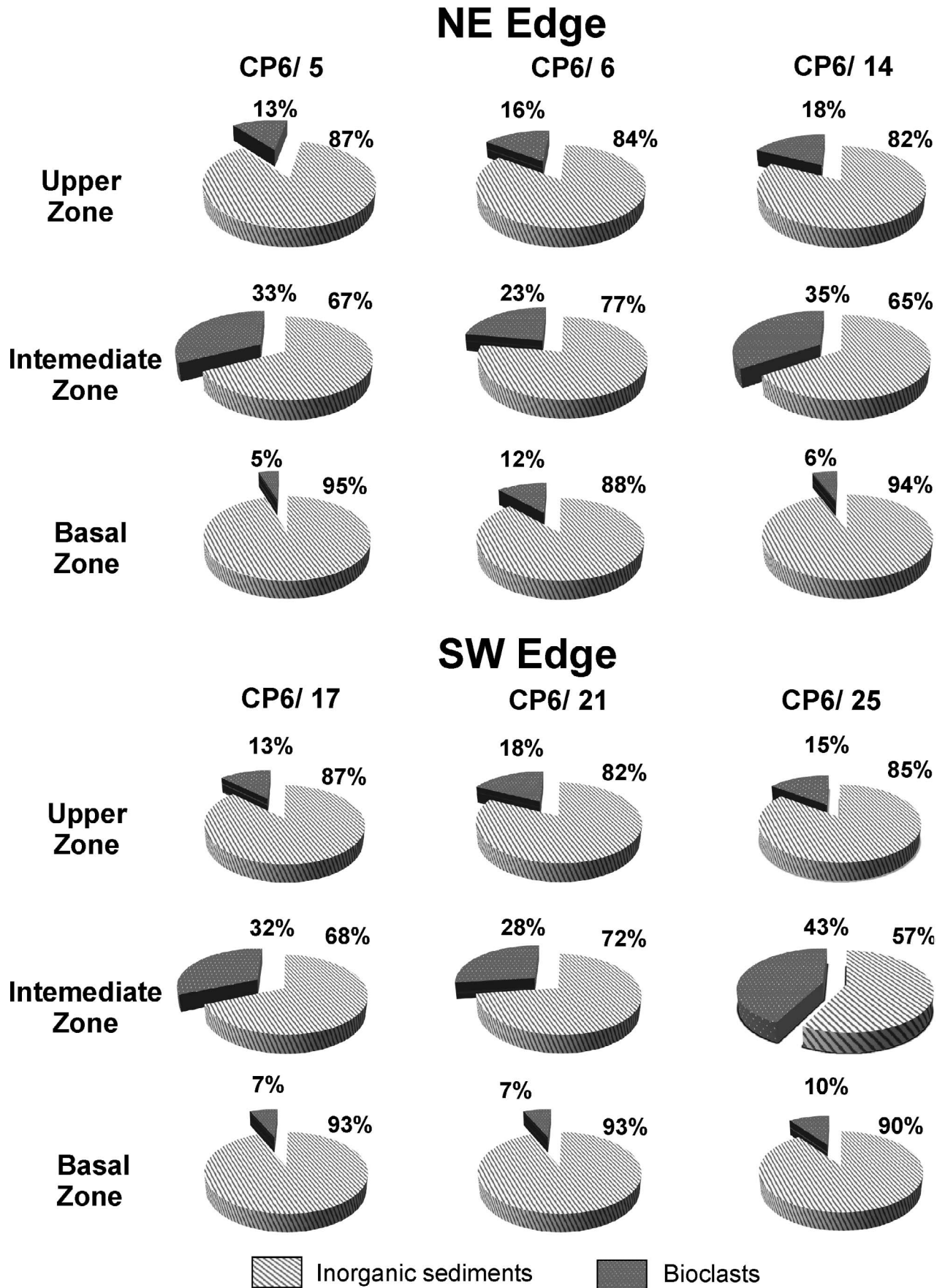7% / 93% 7% / 93% 10% / 90%

Inorganic sediments   Bioclasts

FIG. 8.—Graphs showing percentage of bioclasts and inorganic sediments in each zone of development of microbialites along the SW and NE edges of the Lagoa Salgada.

marine organisms at the base of the microbialite lived when their setting had a direct connection to the sea. Further, they would be unable to survive in the current environmental conditions of the Lagoa Salgada. The metabolic systems varied since the formation of the first laminae of microbialites in Lagoa Salgada, especially those that play a role in carbonate precipitation (Birgel et al. 2015). During open marine conditions, photosynthesis by cyanobacteria dominated and the stromatolitic framework can be observed.

Intermediate Zone.—During the growth of the intermediate zone of the microbialites, fluctuations in sea level recorded by the increase in $\delta^{18}O$ values and seasonal changes may have interfered especially since the late Holocene (Birgel et al. 2015; Angulo et al. 2006). In the period around 2700 cal. yr. BP during which the intermediate zone of the microbialites was formed, southeastern Brazil in general experienced higher rainfall, as shown by palynological studies (Stríkis et al. 2011). Further, the lagoon was experiencing a loss of connection with the sea. The closure of Lagoa Salgada is supported by $\delta^{18}O$ values up to 4‰ lower than marine carbonates (Birgel et al. 2015), suggesting an influence of meteoric water in a closed system (Angulo et al. 2006; Stríkis et al. 2011). The variations in $\delta^{13}C$ indicate changes in physicochemical water conditions related to water-level fluctuations during the development of microbialites (Birgel et al. 2015). The progressive enrichment of ^{13}C (Table 1) also is consistent with the loss of connection with the sea. Also, photosynthesizers such as cyanobacteria had a role in the ^{13}C enrichment by phototrophic CO_2 fixation, by incorporating the isotopically heavy dissolved inorganic carbon (DIC) from the water.

In response to all these changes plus the dominance of photosynthesis by cyanobacteria and algae (Srivastava 2002; Silva e Silva et al. 2008), metazoans found better conditions to proliferate in the lagoonal system. This is possibly reflected by a higher occurrence of bioclasts in the intermediate zone of the microbialites (Fig. 8). Here, the thrombolitic framework coincides with the higher incidence of metazoan (bioclasts) in the matrix of microbialites, pointing to a possible relation with the activity of these organisms (Table 3).

Upper Zone.—In the upper zone there is a higher concentration of Mn associated with the dolomitic matrix (Fig. 4C), which is further evidence for changes in the chemical environment of the lagoon. Some fossil microbialite microbiota are thought to have been able to precipitate Fe and Mn oxides, leaving behind a fossil bioherm-type zonation composed of these oxides (Kuleshov 2017). In Lagoa Salgada, the Mn is not distributed in this way in the upper zone of microbialites. In the Francisqui lagoon (located in the Archipelago Los Roques in the Caribbean Sea) local dolomitization would have been favored by the Mn cycle when the microbial mats were buried (Petrash et al. 2015). The proposed model considers that the alkalinity and consequent dolomite formation is generated by coupled Mn-S redox cycling similarly to bacterial sulfate reduction. Thus, in this model the metal cycling would have greater participation in the dolomite formation than the bacterial processes such as sulfate reduction and methanogenesis. This is indicated by the strong correspondence between Mn and dolomite diagenetic growth in Francisqui lagoon. For the Lagoa Salgada, which is a hypersaline lagoon, the fact that Mn is present in the entire matrix of the microbialite top suggests times of anoxia (for example, burial of the microorganisms), which would favor Mn (II) oxidizing bacteria. These microorganisms can be highly active under low-oxygen conditions (Petrash et al. 2015).

Towards the upper zone of the microbialites there is more enrichment of the $\delta^{13}C$ (17.84‰), which means that microbial activity had more influence in the C incorporation, and the system evolved to a closed lagoon with freshwater influence. As a consequence, these changes influenced the microbial activity. One explanation for the high $\delta^{13}C$ values, uncommon for microbial carbonates (up to $+18$‰, Table 1), is associated with the predominance of methanogenesis (Birgel et al. 2015; Vasconcelos and Bahniuk 2015). Once methanogenesis was the predominant microbial activity at the time of upper-zone formation, the hypothesis that the Mn was incorporated *in situ* at the moment of dolomitization (and not diagenetically) cannot be the best explanation for the Mn distribution. Therefore, we suggest that the incorporation of Mn in microbialites of Lagoa Salgada was caused by intra-sedimentary circulating lagoon water, rich in Mn after the increase of the oxidizing conditions in the lagoon. Further, the prevailing freshwater conditions resulted in low sulfate reduction processes, which consequently resulted in low content of sulfate in the upper zone of stromatolites, meaning that methanogenesis was the dominant carbon remineralizing process at periods of low marine influence (Birgel et al. 2015), as during the development of the upper zone. Although methanogenesis can be responsible for dissolution of carbonate minerals by increasing the acidity of the medium, the microbial mats can contribute to the calcification of microbialites by nucleating precipitated minerals in an oversaturated solution (Birgel et al. 2015).

Here, the stromatolitic mesostructure returns in the upper zone of the microbialites coinciding with the lower abundance of metazoans found in the stromatolitic matrix (Table 3, Fig. 8).

Spatial Distribution of Biofacies

Field visits in October 2009, May 2010, September 2010, and October 2011 confirmed that the conditions of the Lagoa Salgada in 2009, when the QuickBird satellite images were obtained (Fig. 1), were similar to those recorded in 2004 and no change had taken place. The images were essential for the interpretations regarding the differentiated distribution of the biofacies along the edges of the lagoon.

Today, the SW margin is located farther away from the Atlantic coastline. In consequence, the microbialites experience much different hydrodynamic and salinity conditions. With the historical shoreline regression and the closing of the lagoon, significant dynamic and chemical changes took place and affected the growth of these structures (Birgel et al. 2015). At the same time, the lagoon was increasingly colonized by non-lithifying microbial mats (Angulo et al. 2006; Toledo et al. 2009) that are more resistant to the current physicochemical conditions. Currently, the microbial diversity, both in microbial mats and in stromatolites, is composed of several families of cyanobacteria, such as Chroococaceae, Xenococcaseae, Dermocarapaceae, Mycroccystaceae, Oscillatoriaceae, and Enthophysalidaceae, some green and crysophyte and algae, among others (Srivastava 2002). Silva e Silva et al. (2008) identified 21 species of cyanobacteria, include *Aphanothece stagnina* (Sprengel) A. Braun 1863 and *Microcoleus chthonoplastes* (Thuret) Gomont 1892. In general, the majority of these species are tolerant of hypersalinity and other extreme conditions.

The depositional facies of Lagoa Salgada (Fig. 2) is composed of carbonate-cemented structures (microbialites) and two types of non-cemented microbial mats (planar and cauliflower-type), surrounded by the background sediments. The shape of the detrital mineral grains (subrounded to subangular) suggest a high maturity of the deposits, likely due to abrasion by long-time reworking and back and forth transport of the grains. Indeed, the lagoon was once connected with the Paraíba do Sul River, which explains this high sediment maturity. The biofacies and background sediments do not show any specific correlation in their spatial distribution in the lagoon.

There is a predominance of inorganic sediments in both margins, but the participation of microgastropods is also high. This means that these metazoans have been successful in colonizing the environment from a long time ago to the present day, since they are still found alive in the lagoon, especially in ephemeral water pools and among live microbial mats. The S edge of the lagoon is dominated by non-cemented microbial mats whereas microbialites are very scarce. On the basis of QuickBird satellite images

and field visits, one reason for the rarity of microbialites on the S edge is the increased suspension load of the water, which prohibits the significant carbonate mineral formation necessary for a vertical build-up. The cause of cessation of mineralization may also be a change in local lagoonal water chemistry towards a higher salinity and lower input of carbonate. At times, the water in the lagoon may be subject to some turbulence (for example during strong winds, storms, etc.) so that sediment grains are jetted upward and trapped in the framework of the microbialites. Trapping and binding by the microbes and extracellular polymeric substance (EPS) themselves likely did not play any role in this type of intra-frame sediment enrichment.

The non-cemented microbial mat biofacies (NC) in the lagoon includes both the non-cemented planar microbial mats (NC-PM) and the non-cemented cauliflower-type microbial mats (NC-CM). The arrangement of different types of microbial mats into a lateral succession dependent on the morphological surface relief is called biofilm catena (Noffke 2003, 2010). Microorganisms arrange certain mat types favoring specific conditions of hydraulic dynamics and composition of the sediments. In Lagoa Salgada, the two types of microbial mats are distributed differently in the SW and S margins of the lagoon (Fig. 2). According to the different spatial distribution of the biofacies in each margin, the mat succession of the SW margin was called biofilm catena A (Fig. 2A, B) and the one in the S margin, biofilm catena B (Fig. 2C, D). In the S margin the planar microbial mats are thicker; cauliflower-type microbial mats are more abundant. Normalized Division Vegetation Index (NDVI) images (Fig. 2E) show that the intensity of the microbial photosynthesis is higher than in the SW part of the lagoon. The SW margin includes thinner, planar microbial mats and lower amounts of cauliflower-type microbial mats. The establishment of the two biofilm catenae reflects the currently dynamic conditions at the two lagoon margins. The S margin presents calm water conditions, lower depth, and less wave influence, which foster the development of microbial mats; in the SW margin, higher wave and current energy and greater water depth are prohibitive to mat development.

External factors, such as the physical and chemical conditions of the water (indicated by the increase in the $\delta^{13}C$ values), the evolution in the sedimentological dynamics of the lagoon during its origin, variations in the depth and in the sediment influx were determinant for the development, or not, of the microbialites along the different edges of the lagoon. A good indication of this is the non-development of the bioconstructions at the NE and S edges of the lagoon, where the sedimentary dynamics (there is a tendency for more sediment accumulation on these edges) are different from the other edges, in which the microbialites are found, as can be observed in Figure 2. In turn, the changes in water chemistry also reflect on the distribution and abundance of metazoans along the three zones of development of microbialites, as can be observed in Figure 8.

Possible Metazoan Influence on Microbialites and Microbial Mats

The species composition of the bioclasts (skeletal grains) in the biofacies CC, NC-PM, and NC-CM show common biota (Table 2), but differences in abundance, especially between the three zones of development of microbialites, the CC biofacies (Fig. 8). A more diverse population of species is observed in the background sediment of the microbialite voids, such as several species of foraminifers (Table 2) and some species of crustaceans (Gammaride and Tanaidaceae). However, with exception of those bioclasts found in the microbialite matrix and microbial mats, it is noteworthy that the bioclasts belong to organisms whose presence may correspond to different occupation events and/or deposition. Thus, the ecological relation between the Metazoa and the former microbial mats can be inferred from the distribution of biota in microbialite laminae (Table 2). An example of this would be skeletal material of grazers such as *Heleobia australis* found encrusted in the microbialite matrix. Other metazoans such as crustacea have contributed to the production of

fecal pellets, now forming peloids, which were found in the all microbialites of the carbonate-cemented facies (CC).

Some loose bioclasts (e.g., some foraminifers, broken shells of microgastropods, and continental bioclasts, such as plant remnants) occupying the cavities of the microbialites may have been transported to the location by turbulence during more energetic events, like storms. In other cases, however, they may record former Metazoa that occupied the cavities as opportunists for protection or breeding (e.g., crustaceans, Tanaidaceae) or foraging (e.g., *Heleobia australis* and ostracods) at any time without influence of transport. The layer-bounded distribution of encrusters like barnacles and bryozoans indicates specific periods of proliferation of these organisms, perhaps the result of past variations of the water level of the Lagoa Salgada.

In the non-cemented microbial mat-biofacies, the microgastropod shells, ostracods, and foraminifera may have coexisted with the microbial mat as "host." Some of the metazoan species, such as ostracods and *Heleobia australis*, are microalgae foragers living off benthic microalgae on the tops of living microbial mats. Some bioclasts composed of seeds and gyrogonites may have been transported to the sites where mats were growing and been encompassed by the structure during its growth. The concentration of some intact metazoan skeletal grains, such as complete ostracods shells in layers within microbial mats, may point towards specific time periods that fostered proliferation of these organisms. The layers, however, appear too irregular to be considered the result of any seasonality.

Holocene microbialites from other locations worldwide, such as for example areas of the Exuma Cays in the Bahamas, the coast close to Port Elizabeth in South Africa, and shores of Lake Clifton and in Shark Bay in Australia, include skeletal grains as well. Also Metazoa are typically co-occurring, such as foraminifera, gastropods, bivalves, ostracods, bryozoans, and polychaetes (Reid and Browne 1991; Reid et al. 1995, 2003; Konishi et al. 2001; Plasnavsky and Ginsburg 2009; Jahnert and Collins 2012; Rishworth et al. 2016). The crustaceans of the order Tanaidaceae found in the microbialites in the Lagoa Salgada also were observed from microbialites in Porth Elizabeth (Rishworth et al. 2016). Rishworth et al. (2016) suggest that certain serpulids use the microbialites as a refuge. In the Lagoa Salgada, like in the locations above, bioerosion was caused by this burrowing infauna. The abundance of organic matter and benthic microalgae (Srivastava 2002) in the Lagoa Salgada provided excellent living conditions to metazoans. In addition, some species such as the crustaceans of the order Tanaidaceae may have used the void-rich microbialites as good breeding sites and shelter against predation (Johnson and Attramadal 1982). Grazers that feed on microalgae colonizing the microbialites, such as microgastropods *(Heleobia australis)*, crustaceans (Gammaridae, ostracods), and possibly foraminifera, may contribute to bioerosion traces too.

The occurrence of the foraging metazoans, especially those filling the microbialite pores and the carbonate matrix (Table 2), point towards the predation of the microorganisms which compose the microbial mats and the stromatolites. These organisms have contributed mainly to the change in the stromatolite framework, as can be seen in the intermediate zone. In this zone it is possible to observe that the thrombolitic mesostructure coincides with the greatest abundance of bioclasts (Fig. 8), especially those grazers and foraging species, such as ostracods. Most of the foraminifera genera found in the microbialites laminae and filling voids have the detritivorous and/or herbivorous habit, and also are tolerant to hypersalinity (Murray 1991), which makes the Lagoa Salgada an ideal environment for the proliferation of this biota. In the intermediate zone, the abundance and type of prevalent macrobiota (herbivorous, grazers, and detritivorous) seems to have exceeded the process of trapping and binding of sediments to form the stromatolitic laminae, sufficiently to change the mesostructure (the framework), but not to stop the growth of bioconstructions. In this zone, the microbialite mesostructure shows bioerosion marks and a less preserved horizontal lamination. This indicates that the microbial

communities have suffered more bioturbation by metazoans than in the basal and upper zones. The intense activity of metazoans resulted in more interruptions in the formation of parallel laminae of stromatoloid character. In other words, the superior abundance of Metazoa in relation to the development of the other zones was a determining factor for the formation of the thrombolitic structure that predominates in the intermediate zone of the microbialites.

During the development of upper zone of microbialites, the changes in the metabolic function of microbiota in the Lagoa Salgada (such as the increase of methanogenesis) had consequences for the macrobiota too. One of the consequences of methanogenesis predominance was the decrease in food availability (microalgae and cyanobacteria) for detritivorous and/or herbivorous metazoans and, besides, the methane can be toxic for most of these species (Warren et al. 2017). A hostile environment for the proliferation of metazoans may have led to a decrease in predation, which can explain the decrease in abundance of metazoans in upper zone. This favored the change in the framework of microbialites in the upper zone, which returned to the stromatolitic structure.

CONCLUSIONS

The formation of Lagoa Salgada has been associated with coastal-plain evolution, with regressive processes which caused several variations in the water level and consequently, in the physicochemical conditions during the formation of the lagoon. Hence, all these variations are reflected in the macrobiota and microbiota that colonized the lagoon throughout its evolution. The stromatolites recorded all the changes in its isotopic signature, in its composition of bioclasts, and especially in its framework. It is possible to distinguish three zones of development of the bioconstructions, which reflect the consequences of progressive paleo-environmental changes. According the $\delta^{13}C$ and $\delta^{18}O$ values, plus the serpulides tubes firmground, the basal zone of the microbialites began to grow in an open marine setting, with a stromatoloid character and predominance of photosynthesis. During the development of an intermediate zone the lagoon was experiencing a loss of connection with the sea and increased the freshwater influence. The thrombolitic framework of microbialites match with the greater records of the metazoan activity, indicating intense predation of the photosynthesizers. The predominance of photosynthesis was an important factor for the proliferation of metazoans. In the upper zone, the lagoon had already lost its communication with the sea, and the high values of $\delta^{13}C$ indicate changes in the metabolic function of microbiota, from predominance of photosynthesis to predominance of methanogenesis. This also explains the strong presence of Mn distributed in non-bioherm zonation, pointing to diagenetic incorporation. The upper zone is again more of stromatoloid character, likely reflecting the decrease in metazoan predation and the final establishment of the lagoon system as it exists today.

In the Lagoa Salgada, three biofacies dominate the depositional environment: (i) carbonate-cemented microbialites (CC); (ii) cauliflower-type, non-lithified microbial mats (NC-CM), and (iii) planar and non-lithified microbial mats (CC-PM). As a consequence of sedimentary and physical dynamic differences plus the physical characteristics of the surface (relief), the biofacies are arranged into a lateral succession along the various margins of the lagoon, forming a biofilm catena. While the SW margin presents higher wave and current energy and greater water depth, being more prohibitive to mat development (biofilm catena A), the S margin presents calm water conditions, shallower depth, and less wave influence, which favored the development of microbial mats (biofilm catena B).

The sedimentological dynamic in the various margins of the lagoon was the prohibitive factor for the development of microbialites, while the abundance of metazoans was the main factor able to influence the microbialite framework. In other words, the interactions between metazoans and microorganisms appear not to have been prohibitive for the growth of the microbialites, but they were effective in changing the framework of the intermediate zone from stromatolitic to thrombolitic, especially because the highest abundance of metazoans was able to surpass the trapping and binding of sediments to form the stromatolitic laminae.

SUPPLEMENTAL MATERIAL

Supplemental material is available from the JSR Data Archive: https://www.sepm.org/pages.aspx?pageid=229.

REFERENCES

ANGULO, R.J., LESSA, G.C., AND DE SOUZA, M.C., 2006, A critical review of mid- to late-Holocene sea-level fluctuations on the eastern Brazilian coastline: Quaternary Science Reviews, v. 25, p. 486–506.

ARP, G., THIEL, V., REIMER, A., MICHAELIS, W., AND REITNER, J., 1999, Biofilm exopolymers control microbialite formation at thermal springs discharging into the alkaline Pyramid Lake, Nevada, USA: Sedimentary Geology, v. 126, p. 159–176.

AWRAMIK, S.M., 1971, Precambrian columnar stromatolite diversity: reflection of metazoan appearance: Science, v. 174, p. 825–827.

AWRAMIK, S.M., 1982, The origins and early evolution of life, *in* Smith, D.G., ed., The Cambridge Encyclopedia of Earth Sciences: Cambridge UK, Cambridge University Press, p. 349–362.

AWRAMIK, S.M., 1991, Archean and Proterozoic stromatolites, *in* Riding, R., ed., Calcareous Algae and Stromatolites: Berlin, Spring-Verlag, p. 289–304.

BIRGEL, D.P., MEISTER, R., LUNDBERG, T.D., HORATH, T.R.R., BONTOGNALI, A.M., BAHNIUK, A., REZENDE, C.E., VASCONCELOS, C., AND MCKENZIE, J.A., 2015, Methanogenesis produces strong ^{13}C enrichment in stromatolites of Lagoa Salgada, Brazil: a modern analogue for Palaeo-/Neoproterozoic stromatolites?: Geobiology, v. 13, p. 245–266.

BURNE, R.V., AND MOORE, L.S., 1987, Microbialites: organosedimentary deposits of benthic microbial communities: Palaios, v. 2, p. 241–254.

COIMBRA, M.M., CLEVERSON, G.S., BARBOSA, C.F., AND MUELLER, K., 2000, Radiocarbon measurements of stromatolite heads and crusts at the Salgada Lagoon, Rio de Janeiro State, Brazil: Physics Research B, v. 172, p. 592–596.

DELFINO, D.O., WANDERLEY, M.D., SILVA, L.H., SILVA E FEDER, F., AND LOPES, F.A.S., 2012, Sedimentology and temporal distribution of microbial mats from Brejo do Espinho, Rio de Janeiro, Brazil: Sedimentary Geology, v. 263–264, p. 85–95.

DIAS, G.T.M., AND KJERFVE, B., 2009, Barrier and beach ridge systems on the Rio de Janeiro coast, *in* Dillenburg, S., and Hesp, P., eds., Geology and Geomorphology of the Holocene Coastal Barriers of Brazil: New York, Springer, p. 225–252.

D'ORBIGNY, A., 1835, Synopsis terrestrium et fluviatilium molluscorum, in suo per Americam meridionalem itinere: Magasin de Zoologie, v. 5, p. 1–44.

DUPRAZ, C., VISSCHER, P.T., BAUMGARTNER, L.K., AND REID, R.P., 2004, Microbe–mineral interactions: early carbonate precipitation in a hypersaline lake (Eleuthera Island, Bahamas): Sedimentology, v. 51, p. 745–765.

DUPRAZ, R.C., REID, P., BRAISSANT, O., DECHO, A.W., NORMAN, R.S., AND VISSCHER, P.T., 2009, Processes of carbonate precipitation in modern microbial mats: Earth-Science Reviews, v. 96, p. 141–162.

ECKMAN, J.E., ANDRES, M.S., MARINELLI, R.L., BOWLIN, R.P., REID, R.P., ASPDEN, R.J., AND PATHERSON, D.M., 2008, Wave and sediment dynamics along a shallow subtidal sandy beach inhabited by modern stromatolites: Geobiology, v. 6, p. 21–32.

FEDONKIN, M.A., 2003, The origin of Metazoa in light of the Proterozoic fossil record: Paleontological Research, v. 7, p. 9–41.

FLÜGEL, E., 2004, Microfacies of Carbonate Rocks: Analysis, Interpretation and Application: Berlin, Springer-Verlag, 976 p.

GARRETT, P., 1970, Phanerozoic stromatolites: Noncompetitive ecologic restriction by grazing and burrowing animals: Science, v. 169, p. 171–173.

GISCHLER, E., GOLUBIC, S., GIBSON, M.A., OSCHMANN, W., AND HUDSON, J., 2011, Microbial mats and microbialites in the freshwater Laguna Bacalar, Yucatan Peninsula, Mexico, *in* Reitner, J., Quéric, N., and Gernot, A., eds., Advances in Stromatolite Geobiology: Berlin, Springer-Verlag, p. 187–205.

GMELIN, J.F., 1791, Caroli a Linné, systema naturae, Tom. I. Pars VI-Lipsiae (Beer), p. 3021–3910.

HARGRAVE, J.E., HICKS, M.K., AND SHOLZ, C., 2014, Lacustrine carbonates from Lake Turkana, Kenya: a deposicional model of carbonate in an extencional basin: Journal of Sedimentary Research, v. 84, p. 224–237.

IESPA, A.A.C., BORGHI, L., AND IESPA, C.M.D., 2011, O plexo estromatólito–trombólito–oncoide, Lagoa Salgada, RJ, Brasil, *in* Carvalho, S., ed., Paleontologia: Cenários de Vida: Rio de Janeiro, Interciência, v. 3, p. 69–77.

JAHNERT, R.J., AND COLLINS, L., 2012, Characteristics, distribution and morphogenesis of subtidal microbial systems in Shark Bay, Australia: Marine Geology, v. 303–306, p. 115–136.

JOHNSON, S.B., AND ATTRAMADAL, Y.G., 1982, A functional-morphological model of *Tanais cavolinii* Milne-Edwards (Crustacea, Tanaidacea) adapted to a tubiculous life-strategy: Sarsia, v. 67, p. 29–42.

KULESHOV, V., 2017, Manganese carbonates in modern sediments, *in* Maynard, J.B. ed., Isotope Geochemistry: The Origin and Formation of Manganese Rocks and Ores: Amsterdam, Elsevier, p. 5–62.

KONISHI, Y., PRINCE, J., AND KNOTT, B., 2001, The fauna of thrombolitic microbialites, Lake Clifton, Western Australia: Hydrobiologia, v. 457, p. 39–47.

LOPEZ-GARCÍA, P., KAZMIERCZAK, J., BENZERARA, K., KEMPE, S., GUYOT, F., AND MOREIRA, D., 2005, Bacterial diversity and carbonate precipitation in the giant microbialites from the highly alkaline Lake Van, Turkey: Extremophiles, v. 9, p. 263–274.

MACINTYRE, I., PRUFERT-BEBOUT, L., AND REID, R.P., 2000, The role of endolithic cyanobacteria in the formation of lithified laminae in Bahamian stromatolites: Sedimentology, v. 47, p. 915–921.

MARTIN, L., SUGUIO, K., AND FLEXOR, J.M., 1993, As flutuações do nível do mar durante o Quaternário superior e a evolução geológica de deltas brasileiros: Boletim do Instituto de Geociências da Universidade de São Paulo, Publicação Especial, v. 15, p. 1–173.

MONTY, C.L.V., 1973, Precambrian background and Phanerozoic history of stromatolitic communities, an overview: Societé Géologique de Belgique, Annales, v. 96, p. 585–624.

MONTY, C.V.L., 1979, Scientific reports of the Belgian expedition on the Australian Great Barrier Reefs, 1967, Sedimentology: 2, Monospecific stromatolites from the Great Barrier Reef tract and their paleontological significance: Societé Géologique de Belgique, Annales, v. 101, p. 163–171.

MOORE, C.H., 2001, Normal marine diagenetic environments: Sedimentology, v. 55, p. 93–144.

MURRAY, J.W., 1991, Ecology and Paleoecology of Benthic Foraminifera: New York, Longman Scientific Technical, 397 p.

NOFFKE, N., 2003, Epibenthic cyanobacterial communities counteracting sedimentary processes within siliciclastic depositional systems (present and past), *in* Krumbein, W.E., Paterson, D.M., and Zavarzin, G.A., eds., Fossil and Recent Biofilms: Dordrecht, Springer, p. 265–280.

NOFFKE, N., 2010, Geobiology of Microbial Mats in Sandy Deposits from the Archean Era to Today: Berlin, Springer-Verlag, 194 p.

PRATT, B.R., 1982, Stromatolite decline: a reconsideration: Geology, v. 10, p. 512–515.

PESSENDA, L.C.R., AND CAMARGO, P.B., 1991, Datação radiocarbônica de amostras de interesse arqueológico e geológico por espectrometria de cintilação líquida de baixa radiação de fundo: Química Nova, v. 14, p. 98–103.

PETRASH, D.A., LALONDE, S.V., GONZÁLEZ-ARISMENDI, G., GORDON, R.A., MÉNDEZ, J.A., GINGRAS, M.K., AND KONHAUSER, K.O., 2015, Can Mn-S redox cycling drive sedimentary dolomite formation? A hypothesis: Chemical Geology, v. 404, p. 27–40.

PLASNAVSKY, N., AND GINSBURG, R.N., 2009, Taphonomy of modern marine Bahamian microbialites: Palaios, v. 24, p. 5–17.

REID, R.P., AND BROWNE, K.M., 1991, Intertidal stromatolites in a fringing Holocene reef complex, Bahamas: Geology, v. 19, p. 15–18.

REID, R.R., MACINTYRE, I.G., BROWNE, K.M., STENECK, R.S., AND MILLER, T., 1995, Modern Marine Stromatolites in the Exuma cays, Bahamas: uncommonly common: Facies, v. 33, p. 1–7.

REID, R.P., JAMES, N.P., MACINTYRE, I.G., DUPRAZ, C.P., AND BURNE, R.V., 2003, Shark Bay stromatolites: microfabrics and reinterpretation of origins: Facies, v. 49, p. 299–324.

RIDING, R., 2006, Microbial carbonate abundance compared with fluctuations in metazoan diversity over geological time: Sedimentary Geology, v. 185, p. 229–238.

RIDING, R., 2011, Microbialites, stromatolites, and thrombolites, *in* Reitner, J., and Thiel V., eds., Encyclopedia of Geobiology: Dordrecht, Springer, Encyclopedia of Earth Sciences Series, p. 635–654.

RISHWORTH, G.M., PERISSINOTTO, R., AND BIRD, M.S., 2016, Coexisting living stromatolites and infaunal metazoans: Oecologia, v. 181, p. 1–7.

RODRIGUES, M.A., CARVALHO, M.G.P., AND DIAS, G.M.M., 1981, Interpretação paleoambiental das lagoas Salgada e das Ostras (RJ) Brasil, com base em foraminíferos: Congresso Latino-Americano de Paleontologia, Anais, v. 2, p. 893–906.

SAIA, S., PESSENDA, L., GOUVEIA, S., ARAVENA, R., AND BENDASSOLLI, J., 2008, Last glacial maximum (LGM) vegetation changes in the Atlantic Forest, southeastern Brazil: Quaternary International, v. 184, p. 195–201.

SENRA, M.C.E., CONDE, J.N., AND SILVA E SILVA, L.H., 2006, Microbioerosion on shells of *Heleobia australis* (Gastropoda; Rissooidea) from lagoa Salgada, Rio de Janeiro State, Brazil: Instituto de Geociências, Anuário, v. 29, p. 199–209.

SILVA E SILVA, L.H., IESPA, A.A.C., AND DAMAZIO-IESPA, C.M., 2008, Composição dos estromatólitos estratiformes da lagoa Salgada, Rio de Janeiro, Brasil: Instituto de Geociências, Anuário, v. 31, p. 42–49.

SILVA E SILVA, L.H., ALVES, S., MAGINA, F.C., AND GOMES, S., 2013, Composição cianobacteriana e química dos estromatólitos da lagoa Salgada, Neógeno do estado do Rio de Janeiro: Geologia USP, Série, Cientifica, v. 13, p. 96–106.

SPADAFORA, A., PERRI, E., MCKENZIE, J.A., AND VASCONCELOS, C., 2010, Microbial biomineralization processes forming modern Ca:Mg carbonate stromatolites: Sedimentology, v. 57, p. 27–40.

SRIVASTAVA, N.K., 2002, Lagoa Salgada, RJ-Estromatólitos recentes, *in* Schobbenhaus, C., Campos, D.A., Queiroz, E.T., Winge, M., and Berbert-Born, M.L.C., eds., Sítios Geológicos e Paleontológicos do Brasil: Brasília, DNPM/CPRM, Comissão Brasileira de Sítios Geológicos e Paleobiológicos, v. 1, p. 203–209.

STRÍKIS, N.M., CRUZ, F.W., CHENG, H., KARMANN, I., LAWRENCE EDWARDS, R., VUILLE, M., WANG, X., DE PAULA, M.S., NOVELLO, V.F., AND AULER, A.S., 2011, Abrupt variations in South American monsoon rainfall during the Holocene based on a speleothem record from central-eastern Brazil: Geology, v. 39, p. 1075–1078.

TOLEDO, M.B., BARTH, O.M., SILVA, C., AND BARROS, M.A., 2009, Testing multivariate analysis in paleonvironmental reconstructions using pollen records from Lagoa Salgada, NE Rio de Janeiro State, Brazil: Academia Brasileira de Ciências, Anais, v. 81, p. 757–768.

VASCONCELOS, C., WARTHMANN, R., MCKENZIE, J.A., VISSCHER, P.T., BITTERMANN, A.G., AND VAN LITH, Y., 2006, Lithifying microbial mats in Lagoa Vermelha, Brazil: modern Precambrian relics?: Sedimentary Geology, v. 185, p. 175–183.

VASCONCELOS, C., AND BAHNIUK, A., 2015, Microbialitos recentes da região dos lagos, Estado do Rio de Janeiro, *in* Fairchild, T.R., Rohn, R., and Dias-Brito, D., eds., Microbialitos do Brasil do Pré-Cambriano ao Recente: Um Atlas: Rio de Claro, UNES-IGCE-UNESPetro, p. 61–75.

WARREN, L.V., QUAGLIO, F., SIMÕES, M.G., ASSINE, M.L., ALESSANDRETTI, L., LUVIZOTTO, G.L., RICCOMINI, C., AND STRÍKIS, N.M., 2017, A Permian methane seep system as a paleoenvironmental analogue for the pre-metazoan carbonate platforms: Brazilian Journal of Geology, v. 47, p. 722–733.